engineering proceedings

MDPI

*Proceeding Paper*

# Additive Manufacturing of Energy Materials with Composite Structure †

**Svetlana Boshnakova**

Center of Competence "Smart Mechatronic, Eco-and Energy-Saving Systems and Technologies", Technical University Sofia, Branch Plovdiv, 4000 Plovdiv, Bulgaria; boshnakova.sv@bswins.com

† Presented at the 3rd International Online Conference on Energies (IOCEN 2026), 12–15 May 2026; Available online: https://sciforum.net/event/IOCEN2026.

**Abstract**

Waste-to-hydrogen technology requires the involvement of new material development and performance evaluation for additive manufacturing (AM). Metal 3D printing is a very good possible alternative and is delivering results visible in the circular-economy environment. By using the AM technique, complex operations are avoided when combining the individual components, which is a typical disadvantage in obtaining composite materials; such samples are prepared with only one operation from the starting melt, which is chemically defined. Pyrolysis rotary kiln sealing rings are to be upgraded with several different microstructure coatings in order to improve the surface performance. The surface topology is aimed to be fine, dense and smooth. Also, the target characteristics are a low friction coefficient and a high hardness value, suggesting enhanced wear resistance. For elevated temperatures, 900 °C is selected for cobalt-based superalloy Stellite types with particle reinforcement. Two possibilities for advanced materials production are proposed with the Directed Energy Deposition Plasma Arc (DED-arc) and Laser Directed Energy Deposition (DED-LB). The shell of the rotary kiln sealing ring is made of stainless steel as the base, with the coating overlaid. Selected mixtures in powder form with defined composition are applied. For the DED-arc, commercially available Stellite 6 (Deloro Stellite® 6) and 20 vol% WC particles with a grain size of 63–150 μm were employed. For the DED-LB, we employed TRIBALOY® T-800 (Kennametal Stellite™) with 25 vol% TiC and a mesh size of −100/+325 (particle diameter between 45 and 150 μm). After the representative samples were metallurgically bonded with the base stainless steel, the relevant properties were obtained. Manufactured samples are compared in terms of microstructures and mechanical properties. Analysis of structure: Intermetallic carbides that formed on the cobalt basis make the composite harder and increase the plasticity in a defined direction. The hypoeutectic structures of Stellite 6 + 20% WC consist of dendrite and interdendrite eutectic. It is observed that with an increase in WC volume fraction, the size of the dendrites becomes finer, and the amount of eutectic structure is increased. For the TRIBALOY® T-800 with TiC, we obtained relatively smaller grain sizes. The roughness values for the tested samples with WC were initially Ra = 0.8 μm, increasing up to Ra = 3.44 μm after the wear test, whereas for the TiC, they were slightly lower. Microhardness testing revealed increased values compared to the base stainless steels. Advanced sensor analysis with acoustic emission (AE) and electrical contact resistance (ECR) also showed the properties of the new materials. Customizable coatings with tailored properties were deposited by DED-arc and DED-LB. From the tests performed, a new technological procedure for the production of novel pyrolysis rotary kiln sealing rings is proposed. The microhardness, roughness, microstructure and abrasive wear-resistant response of the metallic composite material were examined in order to characterize the stable multiphase system.

Check for updates

Published: 10 September 2026

**Copyright:** © 2026 by the author. Licensee MDPI, Basel, Switzerland. This article is an open access article distributed under the terms and conditions of the Creative Commons Attribution (CC BY) license.

**Keywords:** additive manufacturing; directed energy deposition; composites

## 1. Introduction

Waste-to-hydrogen pyrolysis systems operate at temperatures reaching 900 °C, placing extreme thermal and tribological demands on reactor-side hardware such as rotary kiln sealing rings [1,2]. Rotary kilns are already established reactors for waste pyrolysis; however, the sealing surfaces that maintain process integrity are subject to continuous sliding contact, oxidation and abrasive particulate exposure at these temperatures [3]. Cobalt-based superalloys, notably Stellite 6 and Tribaloy T-800, are attractive candidate coating materials for such service due to their high hardness, oxidation resistance and wear performance across a wide temperature range [4,5]. Directed energy deposition (DED) offers a route to apply these coatings in a single manufacturing operation, avoiding the multi-step fabrication or joining sequences required by conventional surfacing methods [6]. Within DED, arc-based (DED-arc) and laser-based (DED-LB) variants differ fundamentally in energy density, deposition rate and thermal history, producing distinct trade-offs between throughput, dimensional accuracy and microstructural refinement [6,7]. For cobalt alloys specifically, wire arc additive manufacturing (WAAM)-fabricated Stellite 6 has shown primary dendrite arm spacing of 8.28 μm (versus 30.37 μm in castings) and hardness roughly 7 to 8 HRC above that of the cast material, while laser-deposited Stellite 6 layers have reached surface hardness of approximately 335 to 565 HV depending on process parameters [8–10]. Similarly, laser-clad Tribaloy T-800 coatings have achieved hardness near 850 HV and wear coefficients one to two orders of magnitude lower than the substrate, though crack-free deposits require careful control of energy density and substrate preheating [5,11,12].

Despite this growing body of alloy-specific evidence, studies have examined DED-arc and DED-LB routes largely in isolation. Stellite 6 arc-deposition work has focused on bead geometry and dilution control without tribological evaluation [13]. Laser-based Tribaloy T-800 investigations have mapped energy density to cracking thresholds and hardness gradients, yet without an arc-based comparator [11,12]. Broader wire-fed DED reviews confirm that process stability, defect reduction and route selection remain open research questions across alloy families [7,14]. As a result, no direct comparison exists between DED-arc and DED-LB for producing particle-reinforced cobalt-based superalloy coatings on pyrolysis rotary kiln sealing rings, and the relationship between the resulting microstructure and key performance metrics (microhardness, surface roughness, and tribological behavior at 900 °C) remains insufficiently defined.

This knowledge gap carries practical consequences. As waste-to-hydrogen and circular-economy manufacturing systems scale up, there is an immediate need for durable, repairable and manufacturing-efficient high-temperature surface solutions [15,16]. Additive manufacturing is recognized as an enabling technology for component repair and restoration within circular-economy frameworks; however, clear process-property guidance for cobalt hardfacing systems is lacking [15]. Without such guidance, sealing rings risk premature wear and reduced longevity, and engineers lack a rational basis for selecting between available DED routes. Therefore, this study aims to develop and evaluate particle-reinforced Stellite 6 and Tribaloy T-800 coatings produced by DED-arc and DED-LB for pyrolysis rotary kiln sealing-ring upgrading, characterizing microstructure, microhardness, surface roughness, and tribological properties at 900 °C, and proposing a novel single-operation production concept for improved sealing-ring longevity.

https://doi.org/10.3390/engproc2026147020

## 2. Method

Two possibilities for advanced materials fabrication are proposed using DED-arc and DED-LB. The shell of the rotary kiln sealing ring serves as the base, made of stainless steel, with the coating overlaid. Selected mixtures in powder form with defined composition are applied. For the DED-arc, commercially available Stellite 6 (Deloro Stellite® 6, GmbH, Koblenz, Germany) and 20 vol% WC particles with a grain size of 63–150 µm were employed. For the DED-LB, we employed TRIBALOY® T-800 (Kennametal Stellite™, Belleville, ON, Canada) with 25 vol% TiC and a mesh size of −100/+325 (particle diameter between 45 and 150 µm). After the representative samples were metallurgically bonded with the base stainless steel, the relevant properties were obtained.

The new AM materials are intended to restore failed bearings, as shown on Figure 1.



**Figure 1.** Failed bearings for restoration.

The original bearing material is X15CrNi25-21, while the proposed upgrade uses X5CrNi18-10 as the base. In Table 1, the data for both stainless steel materials are compared—for X15CrNi25-21 (1.4845) data according to EN 10095 [17] and X5CrNi18-10 (1.4301) as per EN 10088-3 [18]. It is shown that X15CrNi25-21 and X5CrNi18-10 are similar except for the high-temperature properties. With the overlay, the added layer serves as a barrier and does not allow damaging the softer base.

**Table 1.** Material's characterization—mechanical properties.

| Base Material | Max. Working Temperature (°C) | Yield Strength $R_{p0.2}$ (MPa) | Tensile Strength $R_m$ (MPa) | Hardness HV1 | Rel. Elongation A (%) |
|---|---|---|---|---|---|
| X15CrNi25-21 | up to 1100 | ≥230 | 550–750 | ≤230 | ≥30 |
| X5CrNi18-10 | 800–850 | ≥190 | 500–700 | ≤220 | ≥45 |

This section outlines the proposed procedure for the refurbishment and surface upgrading of defective pyrolysis rotary kiln sealing rings using additive manufacturing (AM) technologies. Experimental work was performed on small samples to ensure the successful execution.

### *2.1. Materials and Substrate Preparation*

The substrate utilized for the deposition process mimics the shell of the rotary kiln sealing ring, manufactured from industrial-grade stainless steel. Prior to cladding, the substrate surfaces were mechanically cleaned and degreased to eliminate contaminants. Two distinct metal matrix composite (MMC) feedstock combinations were prepared:

DED-Arc Feedstock: Commercially available cobalt-based superalloy Deloro Stellite 6 powder blended with 20 vol% of Tungsten Carbide (WC) reinforcing particles (grain size range: 63–150 µm). The chemical composition is given in Table 2.

**Table 2.** The chemical contents of elements in Stellite 6.

| % Content of Elements in Stellite 6 | | | | | | | | |
|---|---|---|---|---|---|---|---|---|
| **Co** | **Cr** | **W** | **C** | **Ni** | **Mo** | **Fe** | **Si** | **Others** |
| Bal. | 28.5 | 4.6 | 1.2 | <2.0 | <1.0 | <2.0 | <2.0 | <1.0 |

DED-LB Feedstock: Cobalt-based TRIBALOY T-800 (Kennametal Stellite™) powder reinforced with 25 vol% of Titanium Carbide (TiC) particles, featuring a mesh size of −100/+325 (particle diameter: 45–150 µm). Table 3 shows the chemical content of the elements in the TRIBALOY T-800.

**Table 3.** The chemical contents of elements in TRIBALOY T-800.

| % Content of Elements in TRIBALOY T-800 | | | | | | | | |
|---|---|---|---|---|---|---|---|---|
| **Co** | **Cr** | **W** | **C** | **Ni** | **Mo** | **Fe** | **Si** | **Others** |
| Bal. | 17 | - | <0.08 | <1.5 | 29 | <1.5 | 3.7 | <1.0 |

### *2.2. Deposition Techniques and Parameters*

Two alternative DED pathways were evaluated to achieve a fine, dense and smooth surface topology capable of withstanding elevated temperatures up to 900 °C:

DED-Arc with the Stellite 6 + 20% WC mixture was deposited using a plasma arc system. This method leverages high deposition rates to build thick, wear-resistant overlay coatings via single-operation melt pool synthesis. The equipment for laser metal deposition was 6-axis Reis Robot Plasmastar Source 250. A Plasmastar 230 MV powder feeder was used for the addition of the particles. The experiments for depositing Stellite 6 + WC via DED-Arc were conducted using an optimized main arc current within the range of 140–160 A. The arc voltage was maintained between 28 and 32 V and was indirectly controlled through adjustments to the arc length and torch standoff distance. Deposition was carried out at a travel speed of 4.5–6.5 mm/s, while the powder feed rate was held constant at 10 g/min. Finally, pure argon was used for arc constriction at a plasma gas flow rate of 2–4 l/min [19].

DED-LB for the TRIBALOY T-800 + 25% TiC powder mixture was processed via a laser-based DED system. The localized laser heat input was optimized to ensure rapid solidification, minimizing the dilution zone while achieving a refined microstructure. The equipment employed was a Rofin Sinar Nd:YAG 2 kW robotized system with powder feedstock. This was a Neodymium-doped Yttrium Aluminum Garnet laser with a wavelength of 1.06 µm. The parameters of the process were specific to each material. The lance setting had a focal distance of 200 mm, and the laser focus spot was around 1 mm. At the power of 1800 W, this corresponds to around 230 kW/cm$^2$. The WC particles were injected in an Ar stream into the tail of the melt pool right after the plasma arc to avoid extra heating in the plasma arc [19].

Both processes were executed under an inert shielding gas atmosphere to prevent oxidation and ensure a stable, defect-free metallurgical bond with the stainless steel base.

### *2.3. Characterization and Performance Evaluation*

Following the deposition process, cross-sections of the representative clad samples were extracted and prepared via standard metallographic routines (mounting, grinding, and polishing). The evaluation matrix comprised the following steps:

Microstructural Analysis: The morphologic evolution, dendrite refinement and distribution of the intermetallic carbides (WC and TiC) within the cobalt matrix were investigated using advanced microscopy techniques.

Mechanical Testing: Surface topology and roughness Ra were quantified both before and after the abrasive wear tests. Vickers microhardness profiles were measured across the coating layer, heat-affected zone and substrate to evaluate the structural integrity.

Advanced Tribological Sensing: Monitoring after the wear testing was conducted using acoustic emission (AE) to detect micro-cracking and deformation mechanisms. Sensors for electrical contact resistance (CR) were also used for characterization of the stability of the multiphase contact interface.

Detailed characterization methods:

Microstructure—the study of microstructure was conducted using an Axiovert 200 MAT microscope (manufactured by Carl Zeiss Microscopy GmbH, Jena, Germany) and an Axiovision camera for recording. Metallographic samples were etched with a mixture of 10 mL $HNO_3$, 20 mL of HCl and 30 mL $H_2O$. The samples were held in the solution for 15 min and then polished.

Roughness—Surface topography and roughness characterization were performed using a Hommel Etamic T8000 high-precision stylus profilometer (manufactured by Jenoptik, Jena, Germany).

Resistance to abrasion measurement—SAR was measured with a Miller tester according to ASTM G75-01 for the abrasive response of the composites, which gives the relevant values for the approved properties compared to the general stainless steel characteristics in abrasive conditions. Tribological testing—A UMT-2M universal mechanical tester (originally CETR, now Bruker, Campbell, CA, USA) system was used for micro-indentation testing and scratch testing. The system is equipped with AE and ECR sensors. Scratch tests were performed with an applied constant force of 6 N along a 5 mm scratch path to analyze the internal and surface changes in the specimen during testing. Acoustic emission functions by detecting elastic waves generated by micro-deformations and early-stage cracks within the material structure. By measuring ECR, it is possible to analyze the evolution of the contact surface, identifying the formation of wear debris or any matter that has been crushed out.

## 3. Results

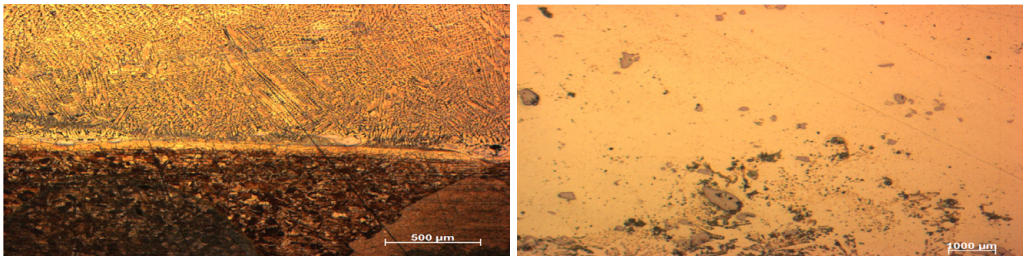
The manufactured samples are compared in terms of microstructures and mechanical properties. For the Stellite 6 + 20% WC over X5CrNi18-10, a total of 18 samples were produced, while for TRIBALOY® T-800 + TiC with base X5CrNi18-10, there were 20 samples. Out of these, 12 representative samples were extracted for the Stellite 6 + 20% WC and the same number for the TRIBALOY® T-800 + TiC. Microidentations were performed at 18 points for the Stellite coating and 47 for the TRIBALOY® T-800 one.

### *3.1. Microstructural Evolution and Phase Analysis*

Analysis of the structure revealed that intermetallic carbides formed on the cobalt basis make the composite harder and increase the plasticity in a defined direction.

The hypoeutectic structures of Stellite 6 + 20% WC consist of dendrite and interdendrite eutectic. It is observed that with an increase in WC volume fraction, the size of the dendrites becomes finer, and the amount of eutectic structure is increased. For the TRIBALOY® T-800 with TiC, relatively smaller grain sizes were obtained. Micrographs of the AM-produced layers are shown in Figure 2.

The metallurgical bonding between the deposited metal matrix composites (MMCs) and the stainless steel substrate exhibited no visible macro-defects, such as delamination or boundary cracking. The microstructural morphology of the DED-Arc track (Stellite 6 + 20 vol% WC) [20] and the DED-LB track (TRIBALOY T-800 + 25 vol% TiC) revealed distinct crystallization pathways.




(**a**) (**b**)

**Figure 2.** AM-produced layers: (**a**) Stelite 6 + WC over X5CrNi18-10; (**b**) TRIBALOY® T-800 with TiC on X5CrNi18-10.

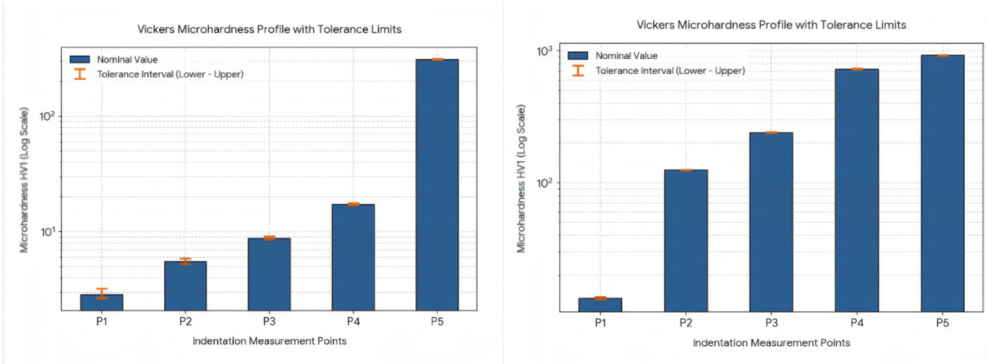
In the case of DED-Arc (Stellite 6 + 20% WC) the result is a hypoeutectic structure composed of fine dendrites and interdendritic eutectic. Microstructural analysis confirmed a characteristic hypoeutectic structure consisting of primary cobalt-rich dendrites and an interdendritic eutectic mixture. The introduction of 20 vol% WC particles acted as nucleation sites during solidification. As a result, an increase in the carbide volume fraction directly correlated with a noticeable refinement of the dendrite size and a higher concentration of the eutectic structure.

For the DED-LB (TRIBALOY T-800 + 25% TiC), a highly refined matrix and uniformly dispersed intermetallic carbides were obtained. The laser-processed tracks demonstrated significantly smaller grain sizes compared to the plasma arc variants. This structural refinement is attributed to the rapid heating and high cooling rates inherent in the DED-LB process.

### *3.2. Microhardness and Surface Roughness*

The mechanical properties of both customizable coatings showed a significant improvement compared to the unclad stainless steel substrate [19–21].

Microhardness: Vickers microhardness profiling across the cross-sections revealed a sharp hardness increase in the coating zone compared to the base metal. The highest microhardness values were recorded in the composite layers due to the combined effects of matrix solid-solution strengthening and carbide dispersion. Specifically, the DED-LB (TiC-reinforced) coating achieved a maximum microhardness of 921 HV1, while the DED-Arc (WC-reinforced) layer averaged 309 HV1. The graphical data is presented in Figure 3.

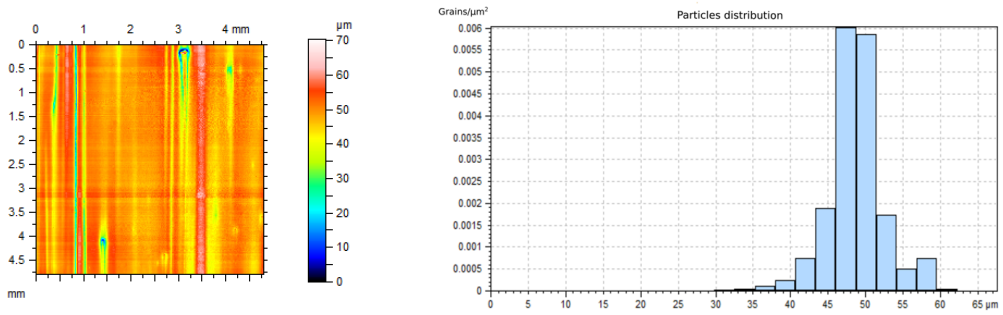



(**a**) (**b**)

**Figure 3.** Hardness data measurements: (**a**) Stelite 6 + WC over X5CrNi18-10; (**b**) TRIBALOY® T-800 with TiC on X5CrNi18-10.

Surface Roughness: The initial surface roughness of the WC-reinforced sample was measured at Ra = 0.8 µm. Following the abrasive wear tests at elevated temperatures,

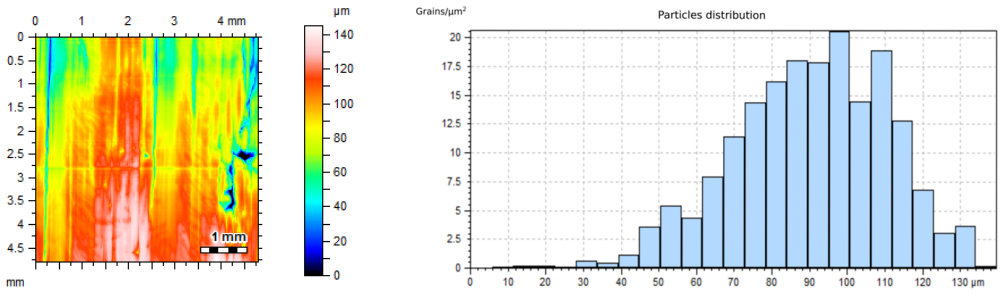
the surface topography shifted and the roughness escalated to Ra = 3.44 µm due to the micro-plowing effects on the softer cobalt matrix. According to ISO 25178 [22], the following parameters were obtained: Sq = 5.18 µm, Ssk = −1.77, Sku = 11.1, Sp = 22.0 µm, Sv = 48.4 µm, Sz = 70.4 µm and Sa =3.44 µm. Figure 4a shows the roughness pattern, and the distribution of the obtained values is given in Figure 4b.




(**a**) (**b**)

**Figure 4.** Roughness measurement data: (**a**) obtained pattern of the roughness; (**b**) distribution of the obtained roughness measurements.

Conversely, the TiC-reinforced DED-LB coating maintained slightly lower roughness values both initially and after wear testing, indicating superior surface topology retention and smoother friction performance. As per ISO 25178, the roughness data is as follows: Sq = 22.8 µm, Ssk = −0.511, Sku = 3.31, Sp = 53.8 µm, Sv = 91.5 µm, Sz = 145 µm and Sa =18.2 µm. Figure 5a shows the roughness pattern, and the distribution of the obtained values is given in Figure 5b.




(**a**) (**b**)

**Figure 5.** Roughness measurement in the DED-LB (TiC-reinforced) sample: (**a**) roughness pattern; (**b**) visual positioning of the data from the measured roughness.

### *3.3. Advanced Sensor Analysis (AE and ECR)*

To evaluate the wear mechanism and the structural response of the stable multiphase systems under thermal stress, acoustic and electrical signals were recorded simultaneously.

Acoustic Emission: The real-time AE signal spectrum successfully identified the distinct deformation stages of the coatings. Low-amplitude acoustic events corresponded to plastic deformation of the cobalt matrix. Periodic high-amplitude bursts were isolated during the wear testing of the DED-Arc samples, signaling micro-cracking at the interface of the larger WC particles (63–150 µm). The DED-LB coating exhibited fewer high-amplitude acoustic events, confirming lower internal stress accumulation and higher crack resistance.

Electrical Contact Resistance: ECR measurements provided deep insight into the structural stability of the contact zone. The ECR values remained stable throughout the evaluation, confirming that the hard intermetallic carbides effectively carried the load. The slightly higher and more consistent ECR values in the TiC coating imply a highly uniform

distribution of non-conductive carbide phases on the sliding surface, proving the formation of a dense, wear-resistant and high-hardness protection layer suitable for high-temperature applications up to 900 °C. The data can be visualized in Figure 6.

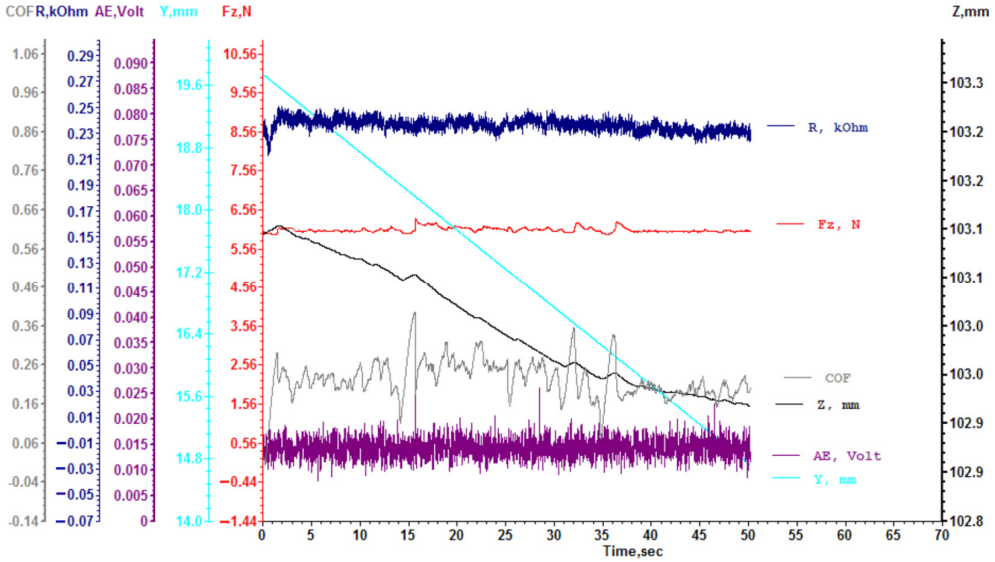



**Figure 6.** Results of the AE and ECR tests: microscratching with a constant force Fz = 6 N over a 5 mm scratching path.

### *3.4. Wear Properties Comparison*

A baseline comparison of the existing and upgraded materials for the sealing ring material is performed [21]. According to the EN 10095 standard, X15CrNi25-21 has a hardness of ≤223 HB, but its wear resistance under dry friction and abrasive conditions at high temperatures is critically low, leading to severe galling. Its mechanical wear resistance degrades drastically at elevated temperatures, making it highly susceptible to severe abrasive wear and plastic deformation. Low surface hardness indicates that the material surface lacks the necessary resistance to withstand the penetration of abrasive dust particles. Furthermore, there is an absence of wear-resistant phases; unlike Stellite, which features hard chromium carbides, and Tribaloy, which contains hard intermetallic Laves phases, the microstructure of X15CrNi25-21 is purely austenitic and completely lacks structural phases capable of mitigating mechanical wear. Unfortunately, samples cannot be extracted from the failed bearing; that is why the comparison is performed using the base material with and without the coatings. The ASTM G75-01 [23] Miller test [21] of the X5CrNi18-10 specimen yielded a specific wear rate of $(8.176 \pm 0.031) \times 10^{-4}$ mm$^3$/Nm; for Tribaloy T-800 + TiC over X5CrNi18-10, the specific wear rate was $(2.639 \pm 0.044) \times 10^{-4}$ mm$^3$/Nm. For Stellite 6 + WC over X5CrNi18-10, the specific wear rate was $(3.178 \pm 0.073) \times 10^{-4}$ mm$^3$/Nm. The wear test demonstrates that the Tribaloy T-800 + TiC over X5CrNi18-10 coating achieves the lowest specific wear rate and minimum cumulative mass loss [19,20]. This result confirms the superior performance of the Tribaloy T-800 + TiC composite compared to Stellite 6 + WC and the baseline X5CrNi18-10 material.

## 4. Discussion

The successful fabrication of Stellite 6 + WC and Tribaloy T-800 + TiC on austenitic stainless steel substrates via Directed Energy Deposition (DED) demonstrates the viability of this process for enhancing the surface properties of critical industrial components—rotary kiln Chesealing rings. Two different variables (different alloys/carbides and different deposition methods) are discussed simultaneously. Both methods and the chosen materials

for manufacturing yield better results in terms of hardness and wear properties than the conventionally used bare X15CrNi25-21. This can be viewed as a limitation of the study but is of significance in practical application, where both DED-Arc and DED-LB show applicability. The selection of alloys/carbides can also be optimized.

## 5. Conclusions

In this study, a new technological procedure using DED pathways was successfully developed and evaluated for the refurbishment and performance upgrading of defective pyrolysis rotary kiln sealing rings. Based on the experimental investigation of the stable multiphase composite coatings, the following conclusions can be drawn:

Successful metallurgical integration: both DED-Arc and DED-LB techniques successfully deposited customizable, defect-free cobalt-based matrix composite coatings onto the stainless steel substrate, ensuring strong metallurgical bonding without boundary cracks or delamination.

Microstructural refinement: the addition of carbide reinforcements significantly improved the crystallization process. The DED-Arc MMC (Stellite 6 + 20 vol% WC) formed a refined hypoeutectic layout with fine dendrites due to WC nucleation effects. The DED-LB MMC (TRIBALOY T-800 + 25 vol% TiC) yielded even smaller grain sizes and high microstructural density, triggered by the rapid solidification inherent to laser processing.

Mechanical and topographical superiority: both coatings exhibited a substantial microhardness increase compared to the unclad stainless steel shell. The initial surface roughness for the WC composite was measured at Ra = 0.8 μm and reached Ra = 3.44 μm post-wear testing, whereas the TiC-reinforced DED-LB variant demonstrated superior surface topology retention with slightly lower roughness metrics.

Advanced mechanistic insights: acoustic emission and electrical contact resistance tracking confirmed that hard intermetallic carbides successfully carried the structural load under high-temperature stress up to 900 °C. The stable ECR signatures and minimal high-amplitude AE crack-events verified that the multiphase systems provide excellent structural stability and low roughness.

The proposed additive manufacturing repair strategy proves to be a viable, high-performance alternative for the circular economy, extending the service life of critical waste-to-hydrogen engineering components.

**Funding:** This research was funded by the European Regional Development Fund under the Operational Program "Scientific Research, Innovation and Digitization for Smart Transformation 2021–2027", Project CoC "Smart Mechatronics, Eco- and Energy Saving Systems and Technologies", BG16RFPR002-1.014-0005.

**Institutional Review Board Statement:** Not applicable.

**Informed Consent Statement:** Not applicable.

**Data Availability Statement:** The data is contained within the article.

**Acknowledgments:** The author would like to express gratitude to University "Prof. Dr. Assen Zlatarov" Burgas, Bulgaria, Technischen Universität Chemnitz, Germany and Open Laboratory on Experimental Micro and Nano Mechanics (OLEM), Bulgaria.

**Conflicts of Interest:** The author declares no conflicts of interest.

## References

1. Foong, S.Y.; Chan, Y.H.; Cheah, W.Y.; Kamaludin, N.H.; Ibrahim, T.N.B.T.; Sonne, C.; Peng, W.; Show, P.; Lam, S.S. Progress in waste valorization using advanced pyrolysis techniques for hydrogen and gaseous fuel production. *Bioresour. Technol.* **2021**, *320*, 124299. [CrossRef]

2. Nandhini, R.; Berslin, D.; Sivaprakash, B.; Rajamohan, N.; Vo, D.N. Thermochemical conversion of municipal solid waste into energy and hydrogen: A review. *Environ. Chem. Lett.* **2022**, *20*, 1645–1669. [CrossRef]
3. Li, A.; Li, X.; Li, S.; Ren, Y.; Shang, N.; Chi, Y.; Yan, J.; Cen, K. Experimental studies on municipal solid waste pyrolysis in a laboratory-scale rotary kiln. *Energy* **1999**, *24*, 209–218. [CrossRef]
4. Wang, L.; Li, D. Effects of yttrium on microstructure, mechanical properties and high-temperature wear behavior of cast Stellite 6 alloy. *Wear* **2003**, *255*, 535–544. [CrossRef]
5. Navas, C.; Cadenas, M.; Cuetos, J.; Damborenea, J.D. Microstructure and sliding wear behaviour of Tribaloy T-800 coatings deposited by laser cladding. *Wear* **2006**, *260*, 838–846. [CrossRef]
6. Ahn, D. Directed Energy Deposition (DED) Process: State of the Art. *Int. J. Precis. Eng. Manuf.-Green Technol.* **2021**, *8*, 703–742. [CrossRef]
7. Casalino, G.; Karamimoghadam, M.; Contuzzi, N. Metal Wire Additive Manufacturing: A Comparison between Arc Laser and Laser/Arc Heat Sources. *Inventions* **2023**, *8*, 52. [CrossRef]
8. Li, Z.; Cui, Y.; Wang, J.; Liu, C.; Wang, J.; Xu, T.; Lu, T.; Zhang, H.; Lu, J.; Ma, S.; et al. Characterization of Microstructure and Mechanical Properties of Stellite 6 Part Fabricated by Wire Arc Additive Manufacturing. *Metals* **2019**, *9*, 474. [CrossRef]
9. Pilehrood, A.E.; Mashhuriazar, A.; Baghdadi, A.H.; Sajuri, Z.; Omidvar, H. Effect of Laser Metal Deposition Parameters on the Characteristics of Stellite 6 Deposited Layers on Precipitation-Hardened Stainless Steel. *Materials* **2021**, *14*, 5662. [CrossRef]
10. Bakhshayesh, M.M.; Khodabakhshi, F.; Farshidianfar, M.; Nagy, Š.; Mohammadi, M.; Wilde, G. Additive manufacturing of Stellite 6 alloy by laser-directed energy deposition: Engineering the crystallographic texture. *Mater. Charact.* **2024**, *207*, 113511. [CrossRef]
11. Xu, X.; Bian, H.; Liu, W.; Xing, F.; Song, B.; Chen, K.; Liu, A. Effect of laser energy density on the microstructure and properties of Tribaloy T-800 coating fabricated by laser cladding on the DZ125 alloy. *Mater. Today Commun.* **2023**, *37*, 107459. [CrossRef]
12. Durejko, T.; Łazińska, M.; Dworecka-Wójcik, J.; Lipiński, S.; Varin, R.A.; Czujko, T. The Tribaloy T-800 Coatings Deposited by Laser Engineered Net Shaping (LENSTM). *Materials* **2019**, *12*, 1366. [CrossRef]
13. Lin, Z.; Ya, W.; Subramanian, V.V.; Goulas, C.; Castri, B.D.; Hermans, M.J.M.; Pathiraj, B. Deposition of Stellite 6 alloy on steel substrates using wire and arc additive manufacturing. *Int. J. Adv. Manuf. Technol.* **2020**, *111*, 411–426. [CrossRef]
14. Özel, T.; Shokri, H.; Loizeau, R. A Review on Wire-Fed Directed Energy Deposition Based Metal Additive Manufacturing. *J. Manuf. Mater. Process.* **2023**, *7*, 45. [CrossRef]
15. Leino, M.; Pekkarinen, J.; Soukka, R. The Role of Laser Additive Manufacturing Methods of Metals in Repair, Refurbishment and Remanufacturing—Enabling Circular Economy. *Phys. Procedia* **2016**, *83*, 752–760. [CrossRef]
16. Kanishka, K.; Acherjee, B. A systematic review of additive manufacturing-based remanufacturing techniques for component repair and restoration. *J. Manuf. Process.* **2023**, *89*, 220–283. [CrossRef]
17. *EN 10095*; Heat-Resisting Steels and Nickel Alloys. CEN: Brussels, Belgium, 1999.
18. *EN 10088-3*; Stainless Steels—Part 3: Technical Delivery Conditions for Semi-Finished Products, Bars, Rods, Wire, Bright Products and Sections of Corrosion Resisting Steels for General Purposes. CEN: Brussels, Belgium, 2014.
19. Boshnakova, S.; Markovska, I.; Rusev, D. SiC and TiC Stainless Steel Based Metal Matrix Composites. *Sci. Work Ruse Univ.* **2015**, *54*, 14–18.
20. Boshnakova, S.; Markovska, I.; Rusev, D. Tribological Behavior of WC Particles Reinforced Surface Metal Matrix Composites Produced by Plasma Melt Injection. In Proceedings of the 4th International Conference on Water, Energy and Environment (ICWEE), Burgas, Bulgaria, 1–3 June 2016.
21. Boshnakova, S. Investigation of New Additive Manufacturing DED Application for Waste-to-Hydrogen Conversion. *Chem. Proc.* **2026**, *20*, 1. [CrossRef]
22. *ISO 25178*; Geometrical Product Specifications (GPS)—Surface Texture: Area. ISO: Geneva, Switzerland, 2021.
23. *ASTM G75-01*; Standard Test Method for Determination of Slurry Abrasivity (Miller Number) and Silt Density Index (SAR Number). ASTM International: West Conshohocken, PA, USA, 2001.


**Disclaimer/Publisher's Note:** The statements, opinions and data contained in all publications are solely those of the individual author(s) and contributor(s) and not of MDPI and/or the editor(s). MDPI and/or the editor(s) disclaim responsibility for any injury to people or property resulting from any ideas, methods, instructions or products referred to in the content.